Double-Barrier Josephson Junctions: Theory and Experiment

A. Brinkman, D. Cassel, A.A. Golubov, M.Yu. Kupriyanov, M. Siegel, and H. Rogalla

***Abstract*—New theoretical and experimental results on double-barrier SIS'IS Josephson junctions are presented (I is a tunnel barrier, S' is a thin film with critical temperature lower than that of S). The previously developed microscopic model for the stationary case, which describes the critical currents in Nb/Al/Nb junctions, is extended to the non-equilibrium regime of finite voltage. In particular, an intrinsic shunting resistance is estimated from I-V curves. We formulate the requirements for interface barriers in order to realize non-hysteretic SIS'IS junctions with high critical current density and I_cR_N products. A comparison with single-barrier SIS junctions with high critical current density is carried out.**

***Index Terms*—Double-barrier, Josephson structures, Non-stationary properties**

I. Introduction

THE recent interest in double-barrier junctions is motivated by the desire to have devices with non-hysteretic current-voltage characteristics, e.g. to apply in large-scale integrated circuits. Double-barrier Josephson junctions are already used in Rapid-Single-Flux-Quantum logic [1] and digital voltage standards [2]. Critical current densities of the order of 1 kA/cm^2 have been obtained [3]-[5]. Non-equilibrium phenomena have been discussed in [6]-[7].

A microscopic model for the stationary properties of double-barrier junctions was developed in [8]-[10]. In this model critical current and normal state resistance are given as function of the critical temperature of the interlayer, interlayer thickness d, and barrier transparencies. Various relations between the electron mean free path l and d were considered. The case of a dirty metal interlayer (l<d) was treated in the framework of the Usadel equations, after deriving the required boundary conditions [8]. In [10], the clean limit (l>d) was studied by solving the full set of Gor'kov equations. It was shown that in both cases the stationary properties of the junction are described by the same effective suppression parameter γ_{eff}:

$$\gamma_{eff} = \frac{d}{\xi_{S'}} \frac{\gamma_{B1}\gamma_{B2}}{\gamma_{B1}+\gamma_{B2}}, \quad \gamma_B = \frac{R_B}{\rho_{S'}\xi_{S'}}, \tag{1}$$

where R_B is the single boundary resistance, d the thickness, $\rho_{S'}$ the resistivity and $\xi_{S'}$ the coherence length of the interlayer. This justifies the use of the diffusive approximation for studying SINIS junctions with a thin normal metal (N) interlayer as will also be done in the work described in the following.

The non-stationary properties were studied so far only in the regime of γ_{eff}<<1. It was shown in [10] that in this case the phase coherence is not lost in the interlayer, i.e. both barriers act effectively as a single one. In this case the concept of Multiple Andreev Reflections (MAR) [11] can be applied to calculate the I-V characteristics of the junctions, which are derived by integrating over the distribution of transmission coefficients of a double-barrier junction. The resulting quasiparticle current-voltage characteristics exhibit the subharmonic structure due to MAR and an excess current I_{ex} at high bias. The harmonic supercurrent components are shown in [10].

From the practical point of view it is desirable to also have a model for large suppression parameters γ_{eff}. In [12] non-stationary properties of SNN' junctions were calculated by making use of the kinetic equations. This work will be extended here for the case of double-barrier SINIS junctions.

The supercurrent and quasiparticle components will be derived, and with these we are able to explain the intrinsic shunting process in double-barrier junctions. Finally it will be shown how the microscopic model is fitted with our most recent experimental data.

II. Theory

A. The kinetic equations

In the regime of low voltages eV<<Δ the phase difference across the junction ϕ=2eVt+ϕ_0 varies slowly in time and the adiabatic approach can be applied. In this case the theory is simplified and the coupled diffusion kinetic equations in the normal metal interlayer have the form [13]:

$$\frac{\partial}{\partial x}\left(D_T \frac{\partial}{\partial x} f_T\right) + \mathrm{Im}\, J_E \frac{\partial}{\partial x} f_L = 0, \quad \frac{\partial}{\partial x}\left(D_L \frac{\partial}{\partial x} f_L\right) + \mathrm{Im}\, J_E \frac{\partial}{\partial x} f_T = 0, \tag{2}$$

Here, the generalized diffusion coefficients are

Manuscript received September 17, 2000. This work was supported by the Dutch Foundation for Fundamental Research on Matter (FOM), the German DFG Project N° Si 704/1-1, by INTAS 97-1712 and ISTC 11-99.

A. Brinkman, A.A. Golubov and H. Rogalla are with the Department of Applied Physics, University of Twente, P.O.Box 7500, 7500 AE Enschede, The Netherlands (telephone: +31 (0)53 4895156, e-mail: a.brinkman @tn.utwente.nl).

M.Yu. Kupriyanov is with Moscow State University, Moscow, Russia.

M. Siegel and D. Cassel are with Forschungszentrum Juelich GmbH, Institut fuer Schicht- und Ionentechnik, Germany

$$D_{T,L}(E,t) = (\mathrm{Re}\, g)^2 \pm (\mathrm{Re}\, f)^2, \tag{3}$$

$f_{L(T)}$ are the longitudinal (transverse) components of the distribution function, and g, f are the normal and anomalous Green's functions in the interlayer, given by

$$g(E,t) = \frac{\gamma_{eff}\dfrac{-iE}{\pi k_B T_c} + g_1\Gamma_{B2} + g_2\Gamma_{B1}}{\sqrt{\tilde{\Gamma}^2 + F_S{}^2\eta^2}}, \tag{4}$$

$$f(E,t) = \frac{F_S\left(\cos\varphi/2 + i\gamma_{-}\sin\varphi/2\right)}{\sqrt{\tilde{\Gamma}^2 + F_S{}^2\eta^2}}, \tag{5}$$

$$g_{1,2}(E,t) = \frac{E \pm eV/2}{\sqrt{(E \pm eV/2)^2 - \Delta_S{}^2}},\ F_S(E,t) = \frac{\Delta_S}{\sqrt{\Delta_S{}^2 - E^2}}, \tag{6}$$

where ϕ=2eVt, $\tilde{\Gamma} = \gamma_{eff} - iE/\pi k_B T + g_1\Gamma_{B2} + g_2\Gamma_{B1}$, η^2=cos^2(ϕ/2)+γ_-sin^2(ϕ/2), $\Gamma_{B1,B2}$=($\gamma_{B1,B2}$)/(γ_{B1}+ γ_{B2}), and γ_-=(γ_{B1}−γ_{B2})/(γ_{B1}+ γ_{B2}). The spectral supercurrent is

$$\mathrm{Im}\, J(E) = \frac{2\pi k_B T}{\xi(\gamma_{B1} + \gamma_{B2})R_n}\frac{F_S{}^2 \sin\varphi}{\sqrt{\tilde{\Gamma}^2 + F_S{}^2\eta^2}}. \tag{7}$$

The distribution functions in the interlayer $f_L(x_{1,2})$, $f_T(x_{1,2})$ are matched at the barriers $x_{1,2}$=±d/2 with the equilibrium distribution functions of the electrodes f_{L0}, f_{T0}

$$\gamma_{B1,2} D_L \frac{\partial}{\partial x} f_{1,2L} = \pm M_{1,2L}(f_{L0} - f_{1,2L}),$$
$$\gamma_{B1,2} D_T \frac{\partial}{\partial x} f_{1,2T} = \pm M_{1,2T}(f_{T0} - f_{1,2T}), \tag{8}$$

where $f_{L0(T0)}$ = [tanh(E+eV/2)/2k$_B$T ± tanh(E-eV/2)/2k$_B$T] / 2, $M_{1,2L(T)}$ = Re $g_{1,2}$ Re g($x_{1,2}$) - (+) Re F_S Re f($x_{1,2}$). The total time-dependent current is given by the sum of quasiparticle (dissipative) and pair components I(t)=I_n+I_S.

The supercurrent component is given by

$$I_s(t) = \frac{1}{R_N}\int_{-\infty}^{\infty} dE\, \mathrm{Im}\, J_E(E,t) f_L(E,t) =$$
$$\frac{1}{R_N}\int_{-\infty}^{\infty}\frac{dE}{2}\mathrm{Im}\, J_E(E,t)\left[(\tanh\frac{E+\frac{eV}{2}}{2k_BT} + \tanh\frac{E-\frac{eV}{2}}{2k_BT})\right], \tag{9}$$

For γ_{eff}>>1 the integral over the spectral supercurrent becomes sinusoidal. Since the bias voltage is assumed to be constant in time, the phase difference ϕ=2eVt evolves linearly in time, thus the supercurrent contribution does not contribute to the dc current at finite voltage.

B. *Quasiparticle current*

The quasiparticle current is given by the expression

$$I_n(t) = \frac{1}{R_N}\int_{-\infty}^{\infty} dE D_T(E,t)\frac{\partial}{\partial_x} f_T(E,t) =$$
$$\frac{1}{R_N}\int_{-\infty}^{\infty}\frac{dE}{2}\frac{\gamma_{B1}+\gamma_{B2}}{\dfrac{\gamma_{B1}}{M_{1T}} + \dfrac{\gamma_{B2}}{M_{2T}}}\left(\tanh\frac{E+\frac{eV}{2}}{2k_BT} - \tanh\frac{E-\frac{eV}{2}}{2k_BT}\right). \tag{10}$$

It follows from (10) that the quasiparticle current has in general a phase-dependent contribution through the coefficients $M_{1,2T}$. Since the phase difference ϕ=2eVt, the quasiparticle current is time-dependent and the dc component is determined by time averaging.

For γ_{eff}<<1 and eV>>Δ, (10) can be decomposed into two terms, representing an SNN' and N'NS junction respectively. Then, an excess current is found. This excess current as function of the asymmetry parameter is plotted in the inset of Fig. 1. This result is reproduced by the MAR formalism [10]. To cover the whole voltage range, the MAR approach has been used and the quasiparticle current as shown in Fig. 1 is obtained [10].

In the case of γ_{eff}>>1, the adiabatic approximation is not necessary, hence, the quasiparticle current for the whole voltage range can be obtained from the kinetic equations. The result is shown in Fig. 2. In this case there is a current deficit at large voltage bias. In the case of symmetric barriers it is obtained that $eI_{def}R_N$=(4/3)Δ, for the completely asymmetric case $eI_{def}R_N$=Δ. The dependency of the current deficit on asymmetry is plotted in the inset of Fig. 2.

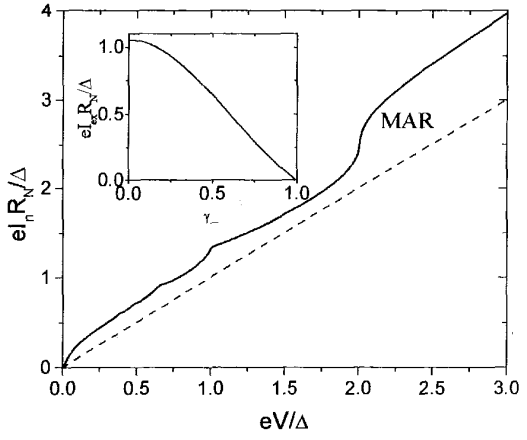

Fig. 1. Quasiparticle current-voltage characteristic for γ_{eff} << 1as obtained from MAR [8]. Inset: the excess current as function of asymmetry.

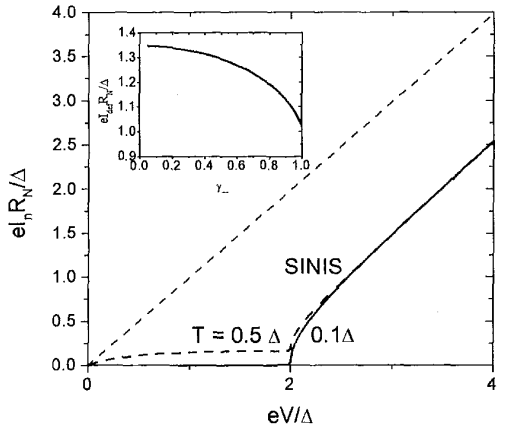

Fig. 2. Quasiparticle current-voltage characteristic for γ_{eff}>>1. Inset: the deficit current as function of asymmetry.

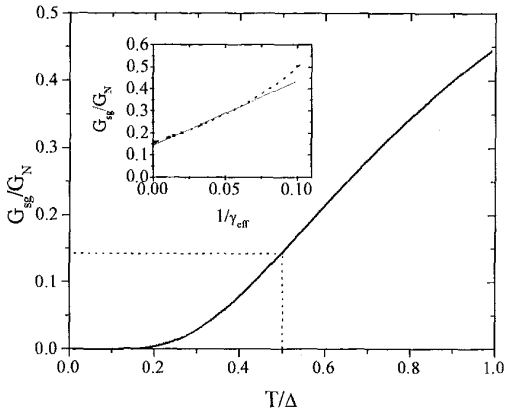

Fig. 3. Subgap conductance as function of temperature (for γ_{eff}>>1) and inset: as function of suppression parameter at fixed temperature (T/Δ=0.5).

C. *Hysteresis*

The Resistively and Capacitively Shunted Junction (RCSJ) model shows how a sinusoidal supercurrent, a linear quasiparticle current and a displacement-current determine the shape of the entire current-voltage characteristic of the junction. The model can also be applied to a non-shunted junction, but then the subgap resistance appears in the expression for the Stewart-McCumber parameter

$$\beta_c = 2\pi \frac{(I_c R_N)^2 C}{I_c \Phi_0} \left(\frac{R_{sg}}{R_N}\right)^2, \qquad (11)$$

C is the capacitance of the junction and Φ_0 the flux quantum. When β_c>1, the corresponding current-voltage characteristic will show hysteresis.

In order to determine the subgap resistance of a double-barrier junction, or its shunting resistance so to say, we notice that there are two contributions to the subgap conductance. The first is purely thermal and can be determined from (10) in the case of barriers with infinitely small transparency. This contribution is plotted in Fig. 3. To get the required average subgap resistance we use the value at eV=Δ. The second contribution to the conductance enhancement is due to the Andreev reflection processes in the interlayer, which is formally introduced by the term Re(f)Re(F_S) in the functions $M_{T1,2}$ in (10). In first order, this contribution is independent of temperature, but it does depend on the suppression parameter, which is shown in the inset of Fig. 3 for a fixed temperature. For the practical range of parameters this means that the contribution is inversely proportional to γ_{eff}. Notice that the cutoff in the inset of Fig. 3 is exactly given by the contribution of thermal quasiparticles.

Let us assume that C=1.5 μF/cm^2 [14], which is the capacitance of two SIS junctions in series, and that it represents a broad range of critical current densities.

Now, the hysteresis parameter can be calculated from (11) together with the expressions for I_c and R_N as function of γ_{eff} from [10]. This is depicted in Fig. 4.

Qualitatively, this curve describes well the experimental data for large critical current densities (> 1 kA/cm^2). For lower critical current densities non-monotonic behavior is expected due to the contribution of anharmonic supercurrent components, which this model did not take into account. Note, that this curve has been calculated at a fixed temperature and would look different if J_c is varied by a temperature change.

Fig. 4 predicts that non-hysteretic double-barrier junctions can be obtained for critical current densities of the order of 10 kA/cm^2 and higher. To make the comparison with SIS junctions, a similar curve has been calculated and plotted in the same Fig. 4. In this calculation it was assumed that C=3 μF/cm^2, I_cR_N=2.0 mV and R_{sg}=2R_N. A bigger subgap resistance will shift the curve even more to the right.

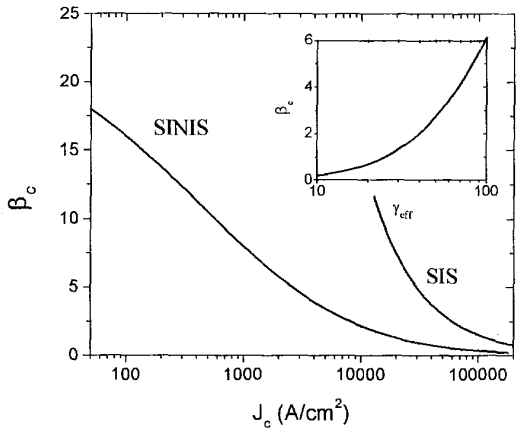

Fig. 4. Stewart-McCumber parameter as function of suppression parameter and critical current density at T/T_c=0.5. SINIS and SIS comparison.

III. Discussion of Experiments

In Fig. 5 the current-voltage characteristic of a Nb/Al double-barrier junction is shown that was fabricated in Jülich, with fabrication parameters similar to those in [15]. In the inset, the modulation with applied field is shown, together with a Fraunhofer fit to show the homogeneity of the current across the junction.

With Zappe's [16] formula for the McCumber parameter

$$\beta_c = \frac{2-(\pi-2)I_c/I_r}{(I_c/I_r)^2}, \qquad (12)$$

a value of 3.0 is obtained for β_c. The McCumber parameter that would follow from our model can be found in Fig. 4 at the corresponding critical current density and has a value within the same order of magnitude.

Figure 6 shows the fit of our theoretical model to the experimental data of different groups. A broad range of suppression parameters is covered. The smallest suppression parameter so far obtained is γ_{eff}=80 [2].

IV. Conclusions

A general theoretical approach to the study of non-stationary properties in double barrier junctions is presented. The results of the model are given for several parameter regimes and describe qualitatively well the intrinsic shunting process in recent experimental data on junctions with high critical current densities [3]-[5]. We predict that an improvement of Nb/Al interfaces up to the level of γ_{eff}~10 will result in $I_cR_N \sim 1$ mV, $J_c \sim 20$ kA/cm^2 and nonhysteretic behavior, $\beta_c \sim 1$ at T=4.2 K.

Acknowledgment

The authors thank D. Balashov, K.K. Likharev, J. Niemeyer and F. Wilhelm for many useful discussions.

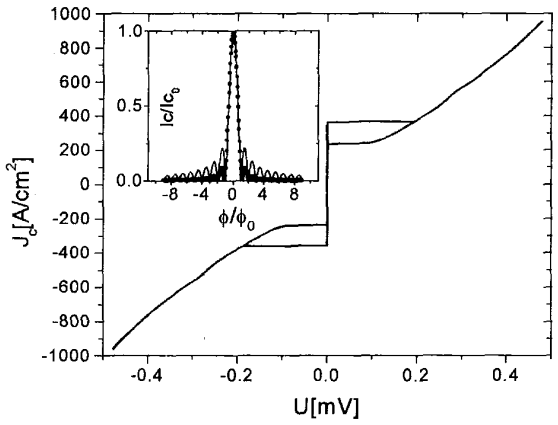

Fig. 5. A hysteretical I-V characteristic of the double-barrier junction with the highest J_c at T=4.2 K. Inset: Critical current modulation by applied field (dots are data, solid line is theoretical fit).

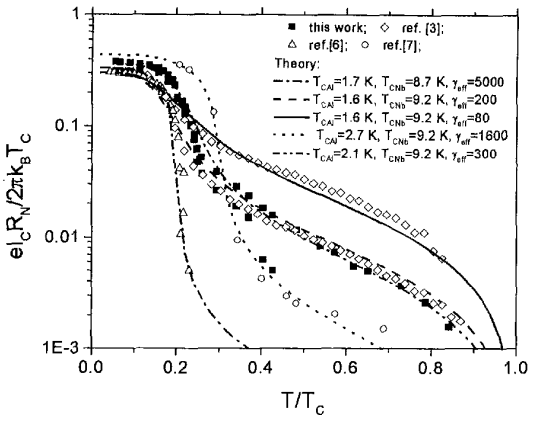

Fig. 6. Fit of the microscopic model for I_c and R_N to the experimental data of various groups. Fitting parameters were T_{cAl}, T_{cNb} and γ_{eff}.

References

[1] D. Balashov, M.I. Khabipov, F-Im Buchholz, W. Kessel, J. Niemeyer, SINIS fabrication process for realizing integrated circuits in RSFQ impulse logic, *Supercond. Sci. Technol.*, vol. 12, p. 864, 1999.

[2] H. Schulze, F. Müller, R. Behr, J. Kohlmann, J. Niemeyer, D. Balashov, SINIS Josephson Junctions for Programmable Josephson Voltage Standard Circuits, *IEEE Trans. Appl. Supercond.*, vol. 9, p. 4241, 1999.

[3] D. Balashov, F-Im Buchholz, H. Schulze, M.I. Khabipov, R. Dolata, M.Yu. Kupriyanov, J. Niemeyer, Stationary properties of SINIS double-barrier Josephson junctions, *Supercond. Sci. Technol.*, vol. 13, p. 244, 2000.

[4] M. Maezawa, A. Shoji, Overdamped Josephson junctions with Nb/AlO_x/Al/AlO_x/Nb structure for integrated circuit application, *Appl. Phys. Lett.*, vol. 70, p. 3603, 1997.

[5] H. Sugiyama, A. Yanada, M. Ota, A. Fujimaki, H. Hayakawa, Characteristics of Nb/Al/AlO_x/Al/AlO_x/Nb Junctions Based on the Proximity Effect, *Japan. J. Appl. Phys.*, vol. 36, p. 1157, 1997.

[6] L. Capogna, G. Burnell, M.G. Blamire, Electronic Cooling in Nb/AlO_x/Al/AlO_x/Nb Double Tunnel Junctions, *IEEE Trans. Appl. Supercond.*, vol. 7, p. 2415, 1997.

[7] I.P. Nevirkovets, Modification of current-voltage characteristics of double-barrier tunnel junctions under the influence of quasiparticle extraction, *Phys. Rev. B*, vol. 56, p. 832, 1997.

[8] M.Yu. Kupriyanov, V.F. Lukichev, Influence of boundary transparency on the critical current of "dirty" SS'S structures, *Sov. Phys. JETP*, vol. 67, p. 1163, 1988.

[9] M.Yu. Kupriyanov, A. Brinkman, A.A. Golubov, M. Siegel, H. Rogalla, Double-barrier Josephson structures as the novel elements for superconducting large-scale integrated circuits, *Physica C*, vol. 326-327, p. 16, 1999.

[10] A. Brinkman, A.A. Golubov, Coherence effects in double-barrier Josephson junctions, *Phys. Rev. B*, vol. 61, p. 11297, 2000.

[11] D.V. Averin, A. Bardas, ac Josephson Effect in a Single Quantum Channel, *Phys. Rev. Lett.*, vol. 75, p. 1831, 1995.

[12] A.F. Volkov, A.V. Zaitsev, T.M. Klapwijk, Proximity effect under nonequilibrium conditions in double-barrier superconducting junctions, *Physica C*, vol. 210, p. 21, 1993.

[13] W. Belzig, F.K. Wilhelm, C. Bruder, G. Schoen, A.D. Zaikin, Quasi-classical Green's function approach to mesoscopic superconductivity, *Superlattices and Microstructures*, vol. 25, p. 1251, 1999.

[14] E. Bartolomé, A. Brinkman, J. Flokstra, A.A. Golubov, H. Rogalla, Double-barrier junction based dc SQUID, *Physica C*, accepted for publication.

[15] D. Cassel, G. Pickartz, M. Siegel, E. Goldobin, H.H. Kohlstedt, A. Brinkman, A.A. Golubov, M. Yu. Kupriyanov, H. Rogalla, Influence of tunnel barriers in Nb/Al_2O_3/Al/Al_2O_3/Nb junctions on transport properties, *Physica C*, submitted for publication.

[16] H. H. Zappe, Minimum current and related topics in Josephson tunnel junction devices, *J. Appl. Phys. 44*, p. 1371, 1973.